

# Context Features Are Cheap: Rank-Aware Decomposition for Efficient Feature Interaction in Recommender Systems

Yevgeny Tkach  
Taboola  
Israel  
yevgeny.t@taboola.com

## ABSTRACT

Modern industrial recommender systems use a deep ranking model to score  $N$  candidates against the same user and context features. Standard implementations broadcast context features early in the forward pass, redundantly computing context-only operations  $N$  times per request. We present a rank-aware decomposition applicable to the dominant interaction mechanisms in modern recommender architectures—Factorization Machine (FM) pairwise products, Deep Cross Network (DCNv2) cross layers, self-attention, and fully connected (FC) projection layers—built on a single algebraic principle: any linear or bilinear operation over a rank-partitioned input admits an exact block decomposition that moves context-only computation from once-per-candidate to once-per-request, identity-equivalent to the original model. Closed-form analysis and controlled ablation verify that savings scale quadratically with the number of context features. Applied to a production DLRM-style ranker without any architectural change, the decomposition increases per-pod throughput by 87.5% (a 47% reduction in peak pod count) at identical model predictions.

The identity-equivalent decomposition applies only at the first layer of cross networks and self-attention, since each layer mixes ranks in its output. To extend savings across depth, we further introduce rDCN, an architectural variant of DCNv2 that maintains rank discipline across depth and matches DCNv2 accuracy within training noise at 67% fewer total FLOPs, and sketch an analogous architectural variant for self-attention.

## KEYWORDS

Recommender Systems, Factorization Machines, Deep Cross Networks, Inference Optimization, Multi-Target Scoring, CTR Prediction

## 1 INTRODUCTION

Industrial recommender systems are typically organized as a two-stage retrieval and ranking pipeline. A cheap retrieval stage narrows a corpus of millions of items down to  $N$  candidates per request; a deep ranking model then scores all  $N$  candidates against the same user and context signals (user profile, browsing history, session state, page context). The ranking stage faces a fundamental tension between model expressiveness and serving cost: as models incorporate richer feature interactions—through pairwise products, cross layers, or attention—the total cost of multi-target scoring grows with both model depth and the number of candidates evaluated per request. For production systems serving billions of daily requests, this cost directly translates into infrastructure footprint.

Most modern ranking architectures—DLRM [14], DeepFM [2], DCNv2 [23], and their variants—share a common structural property: they combine context and target embeddings into a unified feature vector before feeding it through interaction and projection layers. Many implementations broadcast context features to the candidate batch dimension before any computation begins. Downstream operations that involve only context fields—context-only pairwise interactions, linear projections, attention—are redundantly computed  $N$  times. For a model with  $K$  context fields and  $M$  target fields scoring  $N$  candidates per request, the context-context FM interactions alone waste  $(N - 1) \cdot \binom{K}{2} \cdot D$  FLOPs per request, where  $D$  is the embedding dimension.

Recent work on serving optimization addresses this redundancy in fully connected (FC) layers, where the savings scale *linearly* with the number of context fields. In DLRM-style architectures, the dominant industrial paradigm, the bulk of feature-dependent computation occurs in the *interaction* layer, where pairwise combinations cause savings to scale *quadratically*,  $O(K^2)$ . As models incorporate richer context (longer user history, session signals, richer page features),  $K$  grows and the gap between linear (MLP) and quadratic (interaction) savings widens.

*Our contributions are as follows:*

- **A rank-aware decomposition principle.** Any linear or bilinear operation over a rank-partitioned input admits an exact, approximation-free block decomposition. We instantiate this principle across the dominant interaction mechanisms in modern ranking architectures: FM pairwise interactions (as used in DLRM, DeepFM, NFM, PNN), DCNv2 cross layers, self-attention, and FC projection layers.
- **Cost asymmetry.** Rank-aware decomposition makes context features substantially cheaper to serve than target features. This suggests a new tradeoff between adding context vs. target features. Closed-form analysis reveals this asymmetry, and our empirical ablation shows that increasing  $K$  by  $3\times$  reduces RPS by 39%, while a  $3\times$  increase in  $M$  reduces it by 64%.
- **Architecture design principle.** The standard rank-aware decomposition applies only at the first layer in cross networks and attention, because context and target features mix in subsequent layers. This motivates a structural design principle: build recommendation architectures from layers that admit rank-aware decomposition throughout. We propose rDCN, a rank-aware cross network that lifts this restriction across depth, and sketch the analogous decomposable attention layer.

- **Production validation.** Applied without any architectural change to a DLRM-style ranker, the decomposition increases per-pod throughput by 88% (a 47% reduction in pod count) at identical model predictions.

The remainder of the paper is organized as follows. Section 2 reviews feature-interaction architectures and prior work on serving efficiency. Section 3 presents the rank-aware decomposition framework and its instantiations for FM, FC, DCNv2 cross, and attention layers. Section 4 presents rank-aware architectural designs: rDCN and a sketch of rank-aware self-attention. Section 5 presents the FLOP analysis, cross-architecture comparison, controlled ablation, and production deployment results.

## 2 BACKGROUND AND RELATED WORK

### 2.1 Feature Interaction in Recommender Systems

Modern recommender architectures differ primarily in how they combine features into learned interactions. We briefly review the dominant families; Section 3 analyzes each with respect to rank decomposability.

*FM-based neural networks.* A broad family of architectures uses FM-style pairwise embedding products as their interaction layer. DeepFM [2] combines a parallel DNN branch with the bilinear pairwise interactions; NFM [4] introduces bi-interaction pooling followed by an MLP; PNN [17] uses inner/outer product layers feeding an MLP. DLRM [14] is the dominant industrial template: FM-style pairwise interactions followed by a top MLP.

*Cross networks.* DCN [22] and DCNv2 [23] compute feature crosses via residual layers of the form  $\mathbf{x}_{l+1} = \mathbf{x}_l \odot (\mathbf{W}_l \mathbf{x}_l + \mathbf{b}_l) + \mathbf{x}_l$ . GDCN [21] adds information gating. DCNv3 [11] extends the formulation with exponential cross networks.

*Attention-based interactions.* AutoInt [20] applies multi-head self-attention over field embeddings. InterHAT [12] adds hierarchical aggregation. FiBiNET [6] combines SENET-based feature reweighting with bilinear interactions. MaskNet [24] introduces instance-guided masks derived from the full input.

All of the above architectures combine context and target features, creating the redundancy we address.

### 2.2 Making Multi-Target Scoring Lighter

Prior work attacks this cost from several angles, summarized below.

*Structural separation and distillation.* LightSUAN [10] explicitly identifies the cost of multi-target scoring under early-fusion architectures, such as target attention over user-behavior sequences (DIN [28], ETA [16], TWIN [1]) or shared bottom modules, where context-context computations are repeated  $N$  times per request. It addresses this through distillation: a heavier teacher (SUAN, a Stacked Unified Attention Network) is compressed into a lighter student (LightSUAN) that retains early fusion but uses sparse self-attention and parallel-inference batching, trading capacity for efficiency rather than restructuring the fusion mechanism. Two-tower architectures [5, 26] take a more extreme structural path: independent user and item towers with scoring reduced to a dot product,

efficient enough for retrieval over millions of candidates but sacrificing joint user-item features and deep cross-interactions, making them rarely used for final ranking—the regime our work targets. Both lines of work trade expressiveness for serving efficiency. Our rank-aware decomposition contrasts: it is mathematically exact and preserves expressiveness fully, but applies only where context and target features remain separately accessible at the interaction layer. Extending it to early-fused architectures is an open direction for future work.

*Infrastructure-level optimizations.* ROO [3] (Meta, 2025) restructures training data so that each row represents a full user request—one set of user features plus an array of  $N$  candidate items—rather than one (*user, item*) pair per row. This deduplicates user features and embedding lookups across the candidates of a request, yielding 32–100% training throughput gain for late-stage ranking. AIF [9] executes interaction-independent paths (user-only, item-only) asynchronously and approximates the skipped cross-interactions via a learned bridge embedding (+5.80% RPM at pre-ranking with negligible added latency). Both operate at the system level and are complementary to our algebraic approach.

*Model-specific interaction-layer reformulations.* Low Rank FwFM [19] extends the linear-time FM evaluation trick of Rendle [18] to the field-weighted variant: it decomposes the Field-Weighted FM (FwFM [15]) interaction matrix as  $R = U^T \text{diag}(e)U + \text{diag}(d)$  (diagonal plus low-rank), and exploits the resulting structure to compute the context-side sum once per request. Reports 34% average inference latency reduction in a production advertising system. The approach is mathematically elegant but scoped to FwFM and requires an approximation of  $R$ ; it does not extend to FM-based deep networks where pairwise outputs feed downstream layers.

*MaRI.* Closest to our work, MaRI [7] (Kuaishou, 2026) automatically detects redundant FC/MatMul computations via a graph coloring algorithm. When the input to a MatMul has the tiled form  $\mathbf{x} = [\mathbf{x}_u^{\text{tiled}}, \mathbf{x}_i; \mathbf{x}_c]$ , MaRI decomposes the weight matrix to compute  $\text{Tile}(\mathbf{x}_u \mathbf{W}_u) + \mathbf{x}_i \mathbf{W}_i + \mathbf{x}_c \mathbf{W}_c$ , reporting 5.9% hardware savings in Kuaishou production. MaRI’s scope is limited to MatMul(*data, weight*) nodes: savings are linear in the context dimension  $O(d_c)$ , and the analysis does not cover pairwise FM interactions (no weight matrix, so no graph node to detect), cross-network layers, or attention.

## 3 RANK-AWARE DECOMPOSITION

This section presents our first family of contributions: a systematic, *identity-equivalent* block decomposition of feature interaction and projection layers that exploits the rank asymmetry between context and target features in multi-target scoring. Each decomposition presented here produces mathematically identical model output to the standard implementation, just computed more efficiently. We first state the unifying algebraic principle (§3.2), then instantiate it on FM interactions (§3.3), FC layers (§3.4), DCNv2 cross layers (§3.5), and self-attention (§3.6), and conclude with a summary of architectural applicability (§3.7). Section 4 extends this framework with *architectural variants*—designs that trade strict identity equivalence for compounded savings across depth.

### 3.1 Problem Setup and Notation

Consider a recommendation request comprising:

- **Context features**  $\mathbf{c} = \{c_1, \dots, c_K\}$  with embeddings  $\mathbf{e}_{c_k} \in \mathbb{R}^D$ , identical across all candidates in the request. We use “context” to refer to all features that are constant across candidates within a request—both user features (profile, history) and session/page features. Settings in which the same user is scored under multiple distinct impression contexts in one request can be modeled by treating each impression as a separate request, or by introducing an additional rank for the impression axis; we focus on the single-context-per-request case throughout.
- **Candidate items** indexed  $n = 1, \dots, N$ , each with target features  $\mathbf{t}^{(n)} = \{t_1^{(n)}, \dots, t_M^{(n)}\}$  and embeddings  $\mathbf{e}_{t_m}^{(n)} \in \mathbb{R}^D$ . When stacked across candidates, we write  $\mathbf{T} \in \mathbb{R}^{N \times M \times D}$  (or  $\mathbb{R}^{N \times d_t}$  where  $d_t = M \cdot D$  once embedded and flattened) for the rank-3 tensor of all  $N$  candidates’ target features.

The model must produce  $N$  scores  $\hat{y}_1, \dots, \hat{y}_N$ .

*Tensor rank convention.* We distinguish features by the rank of their natural tensor representation:

- **Context embeddings:** rank 2, shape  $[B, D]$ —identical across candidates.
- **Target embeddings:** rank 3, shape  $[B, N, D]$ —vary per candidate.

Here  $B$  is the request batch size (number of requests processed in parallel). In the remainder of the paper we treat  $B = 1$ ; all FLOP calculations and savings scale linearly with  $B$ .

### 3.2 The Unifying Principle

The decompositions in §§3.3–3.6 are all instances of a single algebraic principle. Any operation that is *linear* or *bilinear* in its inputs admits a block decomposition when the inputs partition as  $\mathbf{x} = [\mathbf{x}_c; \mathbf{x}_t]$ .

*Linear case.* For  $f(\mathbf{x}) = \mathbf{W}\mathbf{x}$  with the weight matrix partitioned by input block,  $\mathbf{W} = [\mathbf{W}_c \mid \mathbf{W}_t]$ :

$$\mathbf{W}\mathbf{x} = \mathbf{W}_c\mathbf{x}_c + \mathbf{W}_t\mathbf{x}_t \quad (1)$$

The  $\mathbf{W}_c\mathbf{x}_c$  term is computed once when  $\mathbf{x}_c$  is rank 2 (shared across candidates). This single identity covers FC layers, attention projections, DCNv2’s  $\mathbf{W}_l\mathbf{x}_l$ , and linear gating mechanisms.

*Bilinear case.* For  $f(\mathbf{x}, \mathbf{y}) = \mathbf{x}^T\mathbf{W}\mathbf{y}$  with  $\mathbf{x} = [\mathbf{x}_c; \mathbf{x}_t]$  and  $\mathbf{y} = [\mathbf{y}_c; \mathbf{y}_t]$ :

$$\mathbf{x}^T\mathbf{W}\mathbf{y} = \mathbf{x}_c^T\mathbf{W}_{cc}\mathbf{y}_c + \mathbf{x}_c^T\mathbf{W}_{ct}\mathbf{y}_t + \mathbf{x}_t^T\mathbf{W}_{tc}\mathbf{y}_c + \mathbf{x}_t^T\mathbf{W}_{tt}\mathbf{y}_t \quad (2)$$

The  $\mathbf{x}_c^T\mathbf{W}_{cc}\mathbf{y}_c$  term is computed once. This covers FM interactions, FwFM, bilinear interactions (FiBiNET [6]), outer products (CIN in xDeepFM [13]), and attention scores.

*Standard approach.* Broadcast (tile) context embeddings to rank 3 before any interaction computation, yielding a unified  $[N, (K+M) \cdot D]$  feature tensor. All downstream computation is  $O(N)$  regardless of feature type.

*Our approach.* Defer broadcasting. Compute context-only operations at rank 2, target-only and cross operations at rank 3. Broadcast results only when mixing.

*Where the principle fails.*

- (1) **Mixing operations:** When an operation mixes rank-2 context and rank-3 target inputs into a single output, the output dimensions are rank-mixed and any downstream layer consuming them sees a rank-3 “context” that is no longer pure context. This is the obstacle in FC and DCNv2 cross layers beyond layer 0 (§3.5).
- (2) **Target attention:** DIN [28], TWIN [1], ETA [16]—user representations depend on target by design, so no context-only path exists.

The remaining subsections instantiate this principle on the dominant feature-interaction mechanisms in modern recommender architectures; Table 2 (§3.7) summarizes coverage across architecture families.

### 3.3 FM Interaction Decomposition

A Factorization Machine [18] computes pairwise inner products over all  $K + M$  feature embeddings. We follow the modern industrial formulation in which each  $\mathbf{e}_i \in \mathbb{R}^D$  is the field-level embedding for feature field  $i$ —obtained by looking up the active categorical value (or, for multi-valued fields, by pooling the embeddings of the active values). This subsumes the classical formulation  $\sum_{i < j} \langle v_i, v_j \rangle x_i x_j$  [18] in which  $v_i$  is a latent factor and  $x_i$  a sparse feature value: the field embedding  $\mathbf{e}_i$  here plays the role of  $x_i v_i$  for the active value of field  $i$ , so dense feature values and one-hot indicators are absorbed into the embedding lookup. In line with DLRM-style usage, we treat the FM *output* as the vector of pairwise dot products

$$\text{FM}(\mathbf{e}) = \left[ \langle \mathbf{e}_i, \mathbf{e}_j \rangle \right]_{1 \leq i < j \leq K+M} \in \mathbb{R}^{\binom{K+M}{2}} \quad (3)$$

rather than as the scalar sum in the classical formulation; downstream FC layers consume this vector. The decomposition below operates purely on the  $\mathbf{e}_i$  and is independent of how each embedding is produced.

*Rank-aware decomposition.* Applying the bilinear principle (Eq. 2) to the FM output, we split the pairs into two groups organized by tensor rank:

$$\text{FM}(\mathbf{e}) = \left[ \underbrace{\text{FM}_{\text{ctx}}(\mathbf{c})}_{\text{rank 2, once}} ; \underbrace{\text{FM}_{\text{tgt}}(\mathbf{c}, \mathbf{T})}_{\text{rank 3, per candidate}} \right] \quad (4)$$

where (concatenation is over pairs)

$$\text{FM}_{\text{ctx}}(\mathbf{c}) = \left[ \langle \mathbf{e}_{c_i}, \mathbf{e}_{c_j} \rangle \right]_{1 \leq i < j \leq K} \in \mathbb{R}^{\binom{K}{2}} \quad (5)$$

$$\text{FM}_{\text{tgt}}(\mathbf{c}, \mathbf{T}^{(n)}) = \left[ \langle \mathbf{e}_{t_i}^{(n)}, \mathbf{e}_{c_k} \rangle \right]_{i,k} \left[ \langle \mathbf{e}_{t_i}^{(n)}, \mathbf{e}_{t_j}^{(n)} \rangle \right]_{i < j} \quad (6)$$

$\text{FM}_{\text{ctx}}$  depends only on context embeddings and is identical for every candidate—computed once per request.  $\text{FM}_{\text{tgt}}$  captures every interaction involving *at least one* target field: both target–target pairs and context–target pairs. We group these together because they share the same rank (3), the same per-candidate cost structure, and—as we will show—admit a single asymmetric matmul implementation. This “target-anchored” grouping is structurally

**Table 1: Rank-aware FM decomposition.**

Component	Count	Rank	Per request
FM <sub>ctx</sub>	$K(K-1)/2$	2	Once
FM <sub>tgt</sub>	$KM + M(M-1)/2$	3	$N$ times

the same pattern we will see again in rDCN (§4.2) and in rank-aware attention (§4.3).

*Implementation.* Two building blocks realize this decomposition:

- FM<sub>ctx</sub> computes as the upper-triangle of the  $K \times K$  context inner-product matrix. All operands are rank 2; the result is a rank-2 tensor of size  $\binom{K}{2}$  computed once per request.
- FM<sub>tgt</sub> computes in a single asymmetric matmul: each target field embedding is multiplied against the stacked  $[\mathbf{c}; \mathbf{T}^{(n)}]$  block, covering both the context–target and target–target pairs simultaneously. Context embeddings are broadcast to rank 3 only within this operator.

*FLOP savings.* The standard implementation computes all  $\binom{K+M}{2}$  interactions at rank 3, costing  $N \cdot \binom{K+M}{2} \cdot D$  FLOPs per request. Our decomposition costs  $\binom{K}{2} \cdot D + N \cdot (KM + \binom{M}{2}) \cdot D$ . The absolute savings are:

$$\Delta_{\text{FM}} = (N-1) \cdot \binom{K}{2} \cdot D \quad (7)$$

a quadratic function of  $K$ . The savings fraction of total FM FLOPs is:

$$\frac{\Delta_{\text{FM}}}{\text{FLOPs}_{\text{FM}}^{\text{std}}} = \frac{(N-1) \cdot K(K-1)}{N \cdot (K+M)(K+M-1)} \quad (8)$$

The savings fraction is larger when  $M$  is smaller.

*Applicability across FM variants.* The decomposition above is written for the standard FM formulation but applies unchanged to any architecture whose interaction layer computes pairwise embedding products between feature fields, including DLRM [14], DeepFM [2], NFM [4], and PNN [17]. For field-aware variants such as FFM [8], the same two-way decomposition holds with field-specific embeddings substituted on each side of the inner product.

### 3.4 FC Layer Decomposition

Recommender models commonly stack one or more FC layers after the interaction layer. We treat the first FC layer’s input as a concatenation of a rank-2 context part  $\mathbf{x}_c$  and a rank-3 target part  $\mathbf{x}_t$ —either passed directly or, as in DLRM-style models, produced as the outputs of FM<sub>ctx</sub> and FM<sub>tgt</sub>. The rank-aware FC decomposition is a direct application of the linear case of §3.2 (Eq. 1). The first FC layer exploits the block structure:

$$\mathbf{h} = \sigma([\mathbf{x}_c; \mathbf{x}_t] \mathbf{W} + \mathbf{b}) \quad (9)$$

$$= \sigma(\mathbf{x}_c \mathbf{W}_c + \mathbf{x}_t \mathbf{W}_t + \mathbf{b}) \quad (10)$$

where  $\mathbf{x}_c$  is rank-2,  $\mathbf{x}_t$  is rank-3, and  $\mathbf{W} = [\mathbf{W}_c; \mathbf{W}_t]$  is the kernel partitioned along the input dimension. It is the same  $\mathbf{W}_c$ ,  $\mathbf{W}_t$  split as in Equation 1 (here we write the matrix as concatenated row blocks because the input is concatenated; the algebra is identical).

*RankSplitDense.* We compute  $\mathbf{x}_c \mathbf{W}_c$  once at rank 2, broadcast to rank 3, and add to the per-candidate  $\mathbf{x}_t \mathbf{W}_t$  before applying the nonlinearity. Savings:

$$\Delta_{\text{FC}} = (N-1) \cdot |\mathbf{x}_c| \cdot U \quad (11)$$

where  $U$  is the number of units in the FC layer and  $|\mathbf{x}_c|$  is the size of the rank-2 context input.

*Why only the first FC layer.* After  $\sigma(\mathbf{x}_c \mathbf{W}_c + \mathbf{x}_t \mathbf{W}_t + \mathbf{b})$ , the context and target signals are mixed at every neuron by the nonlinear activation. All subsequent layers operate on fully target-dependent tensors of shape  $[N, U]$ ; no further rank-separated computation is possible without approximation.

When the FC layer sits *downstream of a rank-aware FM*, the context-only FM output  $\mathbf{x}_c = \text{FM}_{\text{ctx}}(\mathbf{c})$  has size  $\binom{K}{2}$  (Eq. 5)—itself quadratic in the context field count. Substituting into Equation 11:

$$\Delta_{\text{FC}} = (N-1) \cdot \binom{K}{2} \cdot U \quad (12)$$

also scales *quadratically* with  $K$ .

Combined with the FM-layer savings of Equation 7, a DLRM-style model thus enjoys quadratic-in- $K$  savings at *both* stages of the forward pass: once in the pairwise interaction layer where the  $\binom{K}{2}$  context-context pairs are computed, and again in the first FC layer where those pairs are projected. This compounding is what makes the optimization so impactful for interaction-heavy models and is absent in MLP-only architectures, where the context input to FC scales only linearly with  $K$ .

### 3.5 DCNv2 Cross Layer Decomposition

A DCNv2 cross layer [23] has the form:

$$\mathbf{x}_{l+1} = \mathbf{x}_0 \odot (\mathbf{W}_l \mathbf{x}_l + \mathbf{b}_l) + \mathbf{x}_l \quad (13)$$

The matmul  $\mathbf{W}_l \mathbf{x}_l$  is precisely the block-output linear case of §3.2 (Eq. 1), with the input partition  $\mathbf{x}_l = [\mathbf{x}_l^c; \mathbf{x}_l^t]$  and the weight matrix partitioned into four blocks:

$$\mathbf{W}_l \mathbf{x}_l = \begin{bmatrix} \mathbf{W}_{cc} & \mathbf{W}_{ct} \\ \mathbf{W}_{tc} & \mathbf{W}_{tt} \end{bmatrix} \begin{bmatrix} \mathbf{x}_l^c \\ \mathbf{x}_l^t \end{bmatrix} = \begin{bmatrix} \mathbf{W}_{cc} \mathbf{x}_l^c + \mathbf{W}_{ct} \mathbf{x}_l^t \\ \mathbf{W}_{tc} \mathbf{x}_l^c + \mathbf{W}_{tt} \mathbf{x}_l^t \end{bmatrix} \quad (14)$$

At layer  $l = 0$  (where  $\mathbf{x}_l = \mathbf{x}_0 = [\mathbf{x}_0^c; \mathbf{x}_0^t]$ ), the terms  $\mathbf{W}_{cc} \mathbf{x}_0^c$  and  $\mathbf{W}_{tc} \mathbf{x}_0^c$  depend only on context features and are computable once per request. Savings fraction for the first cross layer:

$$\frac{d_c^2}{(d_c + d_t)^2} \quad (15)$$

*Why depth matters: the cross-block matmul re-entangles ranks.* The savings above apply only at layer 0. The blocker beyond layer 0 is the same one identified as the second failure mode in §3.2: any linear operation whose inputs include both rank-2 context and rank-3 target produces output rows whose “context dimensions” depend on target features. Concretely, the context-output rows of  $\mathbf{W}_l \mathbf{x}_l$  are  $\mathbf{W}_{cc} \mathbf{x}_l^c + \mathbf{W}_{ct} \mathbf{x}_l^t$ . Once layer 0 emits this rank-mixed output, every subsequent layer’s  $\mathbf{x}_l^c$  is target-dependent, and  $\mathbf{W}_{cc} \mathbf{x}_l^c$  is no longer a rank-2 quantity that can be precomputed. The Hadamard product  $\mathbf{x}_0 \odot (\cdot)$  that follows the matmul is incidental: it preserves rank-3-ness but does not create it. Replacing  $\odot$  with a sum or any other elementwise operator would not recover rank separation, because the rank mixing has already happened in  $\mathbf{W}_l \mathbf{x}_l$  itself. Beyond layer 0,

practical savings diminish to zero. Section 4.2 proposes rDCN, a redesigned cross layer that prevents this re-entanglement.

*Compatibility with DCNv2’s low-rank parameterization.* The original DCNv2 paper [23] also proposes a low-rank parameterization  $\mathbf{W}_l = U_l V_l^T$  with  $U_l, V_l \in \mathbb{R}^{D \times r}$  to reduce parameter count. This composes directly with the rank-aware block decomposition: partitioning the rows as  $U_l = [U_c; U_t]$  and  $V_l = [V_c; V_t]$  induces the block factorization  $\mathbf{W}_{cc} = U_c V_c^T$  (and analogously for  $\mathbf{W}_{ct}, \mathbf{W}_{tc}, \mathbf{W}_{tt}$ ) at no extra parameter cost, and the once-per-request context matmul  $\mathbf{W}_{cc} \mathbf{x}_0^c = U_c (V_c^T \mathbf{x}_0^c)$  remains rank 2.

### 3.6 Attention Layer Decomposition

Attention-based interaction layers (e.g., AutoInt [20], InterHAt [12]) apply self-attention over field embeddings:

$$\text{Attn}(Q, K, V) = \text{softmax}\left(\frac{QK^T}{\sqrt{d_k}}\right)V \quad (16)$$

with  $Q = \mathbf{W}_Q E$ ,  $K = \mathbf{W}_K E$ ,  $V = \mathbf{W}_V E$ , where  $E$  is the stacked field embedding matrix.

*Q/K/V projections decompose directly.* Each projection is a MatMul over concatenated field embeddings and is an instance of Equation 1:

$$\mathbf{W}_Q E = \mathbf{W}_Q [E_c; E_t] = \mathbf{W}_{Q,c} E_c + \mathbf{W}_{Q,t} E_t \quad (17)$$

The context-side projections  $\mathbf{W}_{Q,c} E_c$ ,  $\mathbf{W}_{K,c} E_c$ ,  $\mathbf{W}_{V,c} E_c$  are computed once per request. Target-side projections are per candidate.

*Attention matrix has block structure.* With fields partitioned into context (C) and target (T), the full attention matrix decomposes via the bilinear case (Eq. 2):

$$A = \text{softmax}\left(\begin{bmatrix} Q_c K_c^T & Q_c K_t^T \\ Q_t K_c^T & Q_t K_t^T \end{bmatrix}\right) \quad (18)$$

The  $Q_c K_c^T$  block (context queries attending to context keys) is rank 2 and computed once. The remaining blocks are rank 3.

*Softmax caveat.* The softmax normalization mixes context and target contributions in each row’s denominator. However, the unnormalized context-context block is precomputable, and the row softmax can be assembled via FlashAttention-style block-wise log-sum-exp—combining precomputed context partial sums with per-candidate target contributions in  $O(1)$  extra work per query position.

Savings in attention scale with the fraction of operations involving only context fields, approximately  $K^2 / (K + M)^2$  for the score computation, again quadratic in  $K$ . Due to the final mixing of different ranks in the attention layer, these savings, again, apply only to the first layer.

### 3.7 Applicability Across Architectures

Table 2 summarizes which architecture families admit rank-aware decomposition. The decomposition applies fully to DLRM-style architectures (the dominant industrial paradigm), partially to cross-network-based architectures (limited beyond layer 0 by the cross-block matmul; see §4.2 for the rDCN redesign that lifts this restriction), and to attention-based architectures (with the softmax caveat).

**Table 2: Applicability of rank-aware decomposition to the interaction layer across popular recommender architecture families. The FC stack admits decomposition in all cases and is omitted.**

Architecture	Interaction layer
DLRM [14] / DeepFM [2]	FM pairs: Full
FM [18] / FFM [8] / NFM [4] / PNN [17]	FM/bilinear: Full
FinalMLP [29]	Two-stream: Full
DCNv2 [23] / GDCN [21]	Cross: first layer only
AutoInt [20] / InterHAt [12]	Attention: partial
FiBiNET [6]	Bilinear: partial
MaskNet [24]	Gated: partial
xDeepFM [13]	Outer products: partial
DHEN [27]	Per-submodule

## 4 RANK-AWARE ARCHITECTURE DESIGN

The rank-aware, identity-equivalent decompositions of §3 optimize existing architectures without changing their predictions, but their savings are bounded: in cross networks and attention, each layer mixes ranks in its output, leaving subsequent layers without rank-separated inputs to decompose, so the decomposition applies only at the first layer. This section introduces a complementary class of *architectural variants* that lift this restriction by accepting a constraint on the layer form to avoid rank-mixing. The variants are not identity-equivalent to their standard analogues, but offline evaluation shows accuracy within training noise alongside savings that compound across depth (§5.1).

### 4.1 The Asymmetric Loading Principle

The rank-mixing has a specific source in each architecture: in DCNv2, the off-diagonal  $\mathbf{W}_{ct}$  block maps rank-3 target inputs into the context-dimension half of the layer state; in self-attention, context-field outputs attend over target-field keys and values, again producing context outputs that depend on every candidate.

This motivates the *asymmetric loading principle*: architectures should load context×target interactions onto the target stream only, while the context stream evolves purely through context×context dynamics—so rank separation propagates across the full depth of the stack. Whether this directional constraint meaningfully limits expressiveness is an empirical question that requires hyperparameter tuning of both architectures to compare properly. We instantiate this principle for cross networks (§4.2) and attention (§4.3), with initial offline results for the cross-network instantiation reported in §5.1.

The principle composes with the FC decomposition of §3.4: any rank-aware interaction stack—FM (§3.3) or the architectural variants introduced below—terminates in a rank-2 context representation and a rank-3 target representation, which feed directly into a rank-decomposed FC layer.

### 4.2 Rank-Aware DCN: rDCN

We instantiate the asymmetric loading principle for DCNv2 cross networks by structurally removing the  $\mathbf{W}_{ct}$  block (§3.5) and maintaining two separately-typed states—a rank-2 context stream  $c_l$

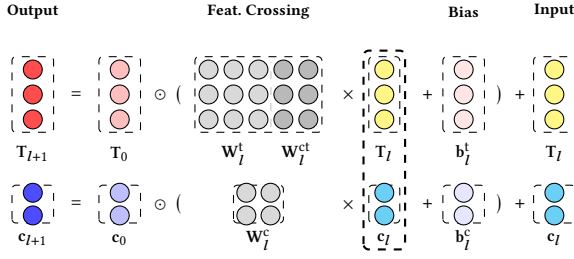


**Figure 1: One rDCN layer. Top row: target stream. Bottom row: context stream. The  $c_l$  tensor is shared between the two streams.**

and a rank-3 target stream  $T_l$ —each updated in parallel by its own DCNv2-style layer:

$$T_{l+1} = T_0 \odot \left( \underbrace{W_l^{ct} c_l}_{\text{rank 2, once}} \oplus \underbrace{W_l^t T_l + b_l^t}_{\text{rank 3}} \right) + T_l \quad (19)$$

$$c_{l+1} = c_0 \odot (W_l^c c_l + b_l^c) + c_l \quad (20)$$

with  $W_l^c \in \mathbb{R}^{D_c \times D_c}$ ,  $W_l^{ct} \in \mathbb{R}^{D_t \times D_c}$ ,  $W_l^t \in \mathbb{R}^{D_t \times D_t}$ , and  $\oplus$  broadcast-and-add along the  $N$  axis. Equivalently, for each candidate  $j$ :  $T_{l+1}^{(j)} = T_0^{(j)} \odot (W_l^{ct} c_l + W_l^t T_l^{(j)} + b_l^t) + T_l^{(j)}$ .

Figure 1 visualizes one rDCN layer using the equivalent block-matrix form for the target stream:  $[W_l^t | W_l^{ct}] [T_l; c_l]$ , where the  $c_l$  slice of the concatenated input also serves as the input to the context stream’s cross layer below.

The context stream (Eq. 20) is a standard rank-2 DCNv2 stack on  $c_l$  alone, evolving the context representation through higher-order  $\text{ctx} \times \text{ctx}$  crosses across depth. The target stream (Eq. 19) is the asymmetric layer: it reads the evolved context  $c_l$  via the rank-2 cross matmul  $W_l^{ct} c_l$  (computed once per request and broadcast along  $N$ ), combines it with the per-candidate state  $W_l^t T_l$ , and applies the Hadamard with  $T_0$ . Since no weight matrix produces context-dimension output from target inputs, the two streams stay rank-2 and rank-3 respectively at every depth. Empirically, this parallel context stream proves essential: removing it causes non-trivial accuracy degradation (Table 3, last DCN row) despite negligible FLOP savings, confirming that the higher-order  $\text{ctx} \times \text{ctx}$  dynamics it captures are load-bearing.

*Parameters per layer.* In the four-block partition of §3.5, rDCN structurally omits the  $W_{ct}$  block (target inputs producing context-dimension output): the context stream reads only  $c_l$ , so no target-to-context coupling is needed. Baseline DCNv2 has  $(D_c + D_t)^2$  weight parameters per layer; rDCN’s three matrices total  $D_c^2 + D_c D_t + D_t^2$ , a saving of  $D_c D_t$  per layer.

*FLOPs per layer.* The context stream contributes  $\Theta(D_c^2)$  (independent of  $N$ ). The target stream contributes  $\Theta(D_t D_c)$  for the once-per-request cross matmul plus  $\Theta(N D_t^2)$  for the per-candidate target matmul. Baseline DCNv2’s per-layer cost, without first-layer rank-aware optimization, is  $\Theta(N D^2) = \Theta(N(D_c^2 + 2D_c D_t + D_t^2))$ , where  $D = D_c + D_t$ . In rDCN this collapses to  $\Theta(D_c^2) + \Theta(N(D_t D_c + D_t^2))$ : the context-driven matmul is removed from the  $N$ -loop entirely,

and the remaining per-candidate work scales linearly in the context dimension where the baseline scales quadratically.

### 4.3 Rank-Aware Attention

The same two-stream design applies to attention-based interaction stacks. As in rDCN, we maintain a rank-2 context stream  $c_l$  and a rank-3 target stream  $T_l$ , each updated by its own attention sub-layer.

*Context stream.* A standard rank-2 self-attention layer over context field embeddings: queries, keys, and values are all drawn from  $c_l$ . Cost per layer is  $\Theta(D_c^2)$ , independent of  $N$ .

*Target-anchored stream.* Queries are drawn only from the target side,  $Q = T_l W_Q$  (rank 3). Keys and values are split by source:  $K^c = c_l W_K^c$  and  $V^c = c_l W_V^c$  at rank 2 (computed once per request), alongside  $K^t = T_l W_K^t$  and  $V^t = T_l W_V^t$  at rank 3. Target queries attend to the concatenation  $[K^c; K^t]$ , and the output is a weighted sum of  $[V^c; V^t]$ . Because context keys and values are produced at rank 2, their projection cost is amortized across all  $N$  candidates.

A production implementation and empirical evaluation are left to future work.

## 5 EVALUATION

We evaluate the rank-aware decomposition in three stages. First, we compare rank-aware component contributions across two architecture families (DCN-style and DLRM-style) on the production dataset, reporting FLOPs and offline metrics (§5.1). Second, we characterize per-pod throughput on synthetic models by sweeping feature counts on production hardware (§5.2). Third, we report production deployment results from Taboola’s recommendation platform (§5.3).

### 5.1 Component Contribution Comparison

Table 3 compares identity-equivalent rank-aware decomposition (§3) and the architectural variant rDCN (§4.2) across two architecture families on our production dataset. Within each family, all configurations share the same model shape; the families themselves operate in different regimes and are listed separately.

Within each family, the identity-equivalent rank-aware decomposition reproduces vanilla predictions to within noise levels ( $\pm 0.0001$  logloss), as expected from a mathematically exact rewriting. The architectural variant rDCN+FC trades strict identity equivalence for a much smaller compute and parameter footprint: it matches DCNv2 within  $\pm 0.0002$  logloss while using 67% fewer total FLOPs and without the  $W_{ct}$  block. The parallel context stream is essential: removing it (last DCN row) yields negligible additional FLOP savings but degrades logloss by  $\sim 0.001$ —an order of magnitude larger than the within-noise differences elsewhere in the table, confirming that the  $c \times c$  interactions the parallel stream captures are load-bearing.

The throughput and production evaluations that follow focus on the DLRM-style architecture currently in production; rDCN has been validated offline above but is not yet deployed online. While rDCN substantially reduces compute within the DCN family (Table 3), the DLRM-style FM+FC variant reaches the same offline accuracy at lower total compute. Looking forward, rDCN’s  $\Theta(D_t D_c)$

**Table 3: Component contributions across architecture families.  $\Delta$  FLOPs are percent change relative to each family’s vanilla baseline. LogLoss is the absolute value with the parenthesized percent change from vanilla. Variant names list the components with rank-aware optimization applied (“+FC” indicates rank-aware FC on top of the interaction-layer variant); rDCN\*\* denotes rDCN with the parallel context stream removed.**

Variant	$\Delta$ FLOPs			LogLoss ( $\Delta$ %)
	Int.	FC	Total	
<i>DCN-style</i> ( $K=26, M=16, d_c=514, d_t=577, L=4$ )				
DCNv2 + FC	-18%	-36%	-20%	0.3876 (+0.02%)
rDCN + FC	-72%	-36%	-67%	0.3877 (+0.05%)
rDCN** + FC	-72%	-36%	-67%	0.3886 (+0.27%)
<i>DLRM-style</i> ( $K=27, M=4, d_c=3456, d_t=512$ )				
FM	-87%	0%	-17%	0.3875 (+0.03%)
FM + FC	-87%	-69%	-73%	0.3875 (+0.01%)

per-layer cost makes expanding context within the DCN family (currently  $d_c=514$  vs. DLRM-style’s 3456) substantially cheaper than DCNv2 admits—an exploration we leave to future work.

## 5.2 Throughput Characterization

We validate the theory empirically on synthetic DLRM-style models (FM interaction layer followed by FC layers), varying one feature-count parameter at a time. Each configuration is built twice—once with the vanilla implementation and once with the rank-aware decomposition—and both are served on the same hardware: a 16-vCPU pod with 16 GiB RAM, pinned to an Intel Xeon Silver 4510 host (Sapphire Rapids, 2.4–4.1 GHz, AMX/AVX-512 VNNI), running TensorFlow Serving 2.x with oneDNN enabled. The client issues 64 concurrent in-flight requests in a closed loop (a new request is dispatched whenever a response returns), and we record the steady-state request rate (RPS) per configuration. We report *normalized RPS*: each measurement is divided by the RPS of the smallest-model vanilla baseline, ( $K = 8, M = 4$ ), so that the baseline reads 1.00 and all other curves can be read relative to it.

*Experiment A: Varying context features  $K$  (with  $M = 4$  fixed).* Figure 2a plots normalized RPS as  $K$  grows from 8 to 24. The vanilla curve degrades steeply (from 1.00 to 0.34), while the rank-aware curve degrades much more gradually (from 1.13 to 0.69), so the rank-aware advantage *widens* from +13% at  $K = 8$  to +105% at  $K = 24$ .

*Experiment B: Varying target features  $M$  (with  $K = 8$  fixed).* Figure 2b plots normalized RPS as  $M$  grows from 4 to 24. Both curves degrade in near-lockstep (vanilla: 1.00 to 0.29; rank-aware: 1.13 to 0.31); the rank-aware advantage stays in a narrow +7–+21% band. As  $M$  grows, target-side compute dominates, so the context-only rank-aware savings become a smaller fraction of total work.

## 5.3 Production Validation

We deployed the DLRM-style FM+FC rank-aware variant (§5.1) online in Taboola’s recommendation platform and compared it

**Table 4: Production deployment results for the DLRM-style ranker. All values are percent change relative to the vanilla baseline. Per-pod RPS is computed at peak traffic under a fixed latency SLA; p50 and p99 are mean latency.**

Variant	RPS/pod	p50	p99
FM rank-aware	+25%	-17%	-26%
FM + FC rank-aware	+87.5%	-30%	-33%

against the vanilla baseline. The production ranking model runs on CPU infrastructure with autoscaled Kubernetes pods; the autoscaler maintains a fixed latency SLA, so per-pod throughput (RPS per pod) is the direct measure of serving efficiency. Table 4 reports per-pod throughput gain and mean latency at peak traffic for the two optimized configurations.

The FM optimization alone increases per-pod throughput by 25%. Adding the FC optimization compounds the gain to +87.5% (equivalently, a 47% reduction in peak pod count). The FC optimization is therefore not merely an incremental refinement over the FM optimization—it captures a meaningful share of the remaining redundancy. This is consistent with the theoretical analysis in §3.4: both stages contribute quadratic-in- $K$  savings that compound across the forward pass.

*Wall-clock latency.* The right two columns of Table 4 report mean p50 and p99 latency. Both percentiles reduce monotonically with more rank-aware optimization, and p99 reduces more than p50, consistent with context-context redundancy disproportionately affecting tail latency in the vanilla implementation.

## 6 CONCLUSION

We presented a rank-aware decomposition for multi-target recommendation scoring built on a single algebraic principle: any linear or bilinear operation over a rank-partitioned input admits an exact block decomposition that moves context-only computation from once-per-candidate to once-per-request. We instantiated this principle across the dominant interaction mechanisms in modern ranking architectures—FM pairwise products, FC projection layers, DCNv2 cross layers, and self-attention—without changing model predictions.

Closed-form analysis and controlled ablation reveal an asymmetry: savings scale quadratically with the number of context features and remain insensitive to target feature count—an asymmetry not available in pure MLP architectures, where FC-layer savings scale only linearly. Applied to a production DLRM-style ranker without any architectural change, the decomposition increased per-pod throughput by 87.5%—a 47% reduction in peak pod count at identical model predictions—while reducing both p50 (–30%) and p99 (–33%) serving latency.

The identity-equivalent decomposition has a structural limit: in cross networks and attention, each layer mixes ranks in its output, so it applies only at the first layer. To propagate rank discipline across the full depth of the stack, we introduced rDCN—an architectural variant of DCNv2 that structurally forbids the off-diagonal target-to-context coupling—and sketched an analogous variant for

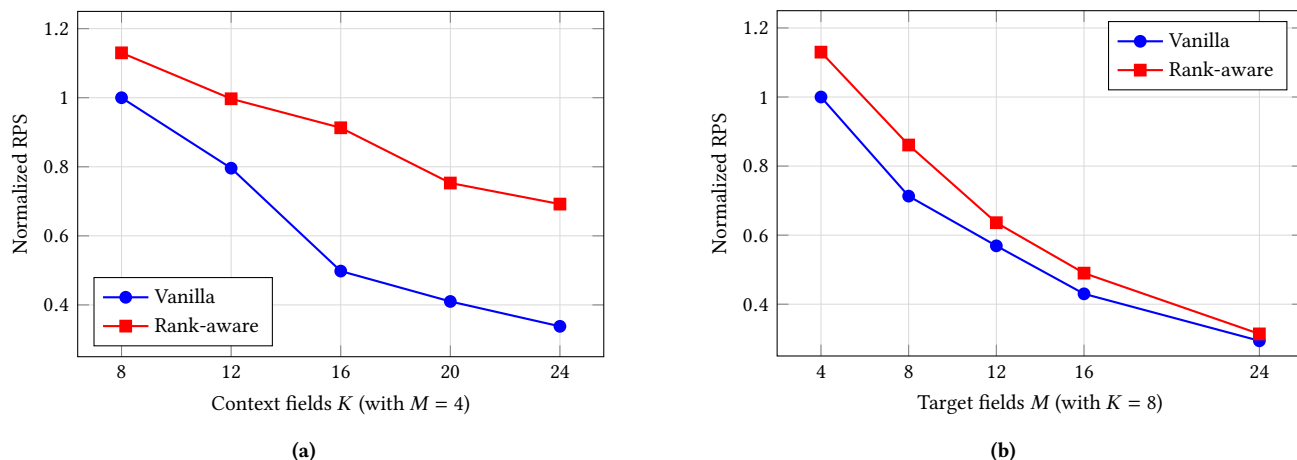


**Figure 2: Throughput normalized to the ( $K = 8, M = 4$ ) vanilla baseline. Left panel (a) varies  $K$  with  $M=4$  fixed; right panel (b) varies  $M$  with  $K=8$  fixed. The vertical gap between the two curves in each panel is the throughput gain delivered by rank-aware decomposition at that configuration.**

self-attention. We validated rDCN offline: it matches DCNv2 accuracy within training noise at 67% fewer total FLOPs.

Two directions remain open. First, online validation: the DCN family’s small per-field context dimension makes rDCN a natural candidate for scaling context substantially beyond what DCNv2 currently admits, and empirical evaluation of the rank-aware attention sketch awaits a production implementation. Second, extending rank-aware approaches to architectures that early-fuse the target into the user-side representation via shared self-attention. Target-attention models (DIN [28], ETA [16], TWIN [1]) are accommodated by the rank-aware attention sketch of §4.3; the harder case is self-attention with target-token injection as in TransAct [25], where the target’s presence in the user-action sequence makes history representations per-candidate at the first layer—breaking rank discipline before any decomposable structure can be applied.

## ACKNOWLEDGMENTS

I thank Shiran Schwartz and Maoz Cohen for their thoughtful feedback on earlier drafts of this work.

## REFERENCES

- [1] Jianxin Chang, Chenbin Zhang, Zhiyi Fu, Xiaoxue Zang, Lin Guan, Jing Lu, Yiqun Hui, Dewei Leng, Yanan Niu, Yang Song, and Kun Gai. 2023. TWIN: Two-stage Interest Network for Lifelong User Behavior Modeling in CTR Prediction at Kuaishou. In *Proceedings of the 29th ACM SIGKDD Conference on Knowledge Discovery and Data Mining (KDD)*.
- [2] Huifeng Guo, Ruiming Tang, Yunming Ye, Zhenguo Li, and Xiuqiang He. 2017. DeepFM: A Factorization-Machine based Neural Network for CTR Prediction. In *Proceedings of the 26th International Joint Conference on Artificial Intelligence (IJCAI)*. 1725–1731.
- [3] Liang Guo, Wei Li, Lucy Liao, Huihui Cheng, et al. 2025. Request-Only Optimization for Recommendation Systems. *arXiv preprint arXiv:2508.05640* (2025).
- [4] Xiangnan He and Tat-Seng Chua. 2017. Neural Factorization Machines for Sparse Predictive Analytics. In *Proceedings of the 40th International ACM SIGIR Conference on Research and Development in Information Retrieval*. 355–364. <https://doi.org/10.1145/3077136.3080777>
- [5] Jui-Ting Huang, Ashish Sharma, Shuying Sun, Li Xia, David Zhang, Philip Pronin, Janani Padmanabhan, Giuseppe Ottaviano, and Linjun Yang. 2020. Embedding-Based Retrieval in Facebook Search. In *Proceedings of the 26th ACM SIGKDD International Conference on Knowledge Discovery & Data Mining*. 2553–2561. <https://doi.org/10.1145/3394486.3403305>
- [6] Tongwen Huang, Zhiqi Zhang, and Junlin Zhang. 2019. FiBiNET: Combining Feature Importance and Bilinear Feature Interaction for Click-Through Rate Prediction. In *Proceedings of the 13th ACM Conference on Recommender Systems (RecSys)*. 169–177. <https://doi.org/10.1145/3298689.3347043>
- [7] Yusheng Huang, Pengbo Xu, Shen Wang, Changxin Lao, Jiangxia Cao, Shuang Wen, Shuang Yang, Zhaojie Liu, Han Li, and Kun Gai. 2026. MaRI: Accelerating Ranking Model Inference via Structural Re-parameterization in Large Scale Recommendation Systems. *arXiv preprint arXiv:2602.23105* (2026).
- [8] Yuchin Juan, Yong Zhuang, Wei-Sheng Chin, and Chih-Jen Lin. 2016. Field-Aware Factorization Machines for CTR Prediction. In *Proceedings of the 10th ACM Conference on Recommender Systems (RecSys)*. 43–50. <https://doi.org/10.1145/2959100.2959134>
- [9] Zhi Kou, Xiang-Rong Sheng, Shuguang Han, Zhishan Zhao, Yueyao Cheng, Han Zhu, Jian Xu, and Bo Zheng. 2025. AIF: Asynchronous Inference Framework for Cost-Effective Pre-Ranking. *arXiv preprint arXiv:2511.12934* (2025).
- [10] Weijiang Lai, Beihong Jin, Jiongyan Zhang, Yiyuan Zheng, Jian Dong, Jia Cheng, Jun Lei, and Xingxing Wang. 2025. Exploring Scaling Laws of CTR Model for Online Performance Improvement. In *Proceedings of the Nineteenth ACM Conference on Recommender Systems (RecSys ’25)*. <https://doi.org/10.1145/3705328.3748046>
- [11] Yan Li, Lingling Zhang, Ziwei Li, Bowei He, Chuhan Wu, Menghui Zhu, Ning Yao, Huifeng Guo, and Ruiming Tang. 2024. DCNv3: Towards Next Generation Deep Cross Network for CTR Prediction. *arXiv preprint arXiv:2407.13349* (2024).
- [12] Zeyu Li, Wei Cheng, Yang Chen, Haifeng Chen, and Wei Wang. 2020. Interpretable Click-Through Rate Prediction through Hierarchical Attention. In *Proceedings of the 13th International Conference on Web Search and Data Mining (WSDM)*. 313–321.
- [13] Jianxun Lian, Xiaohuan Zhou, Fuzheng Zhang, Zhongxia Chen, Xing Xie, and Guangzhong Sun. 2018. xDeepFM: Combining Explicit and Implicit Feature Interactions for Recommender Systems. In *Proceedings of the 24th ACM SIGKDD International Conference on Knowledge Discovery & Data Mining*. 1754–1763. <https://doi.org/10.1145/3219819.3220023>
- [14] Maxim Naumov, Dheevatsa Mudigere, Hao-Jun Michael Shi, Jianyu Huang, Narayanan Sundaraman, Jongsoo Park, Xiaodong Wang, Udit Gupta, Carole-Jean Wu, Alisson G. Azzolini, et al. 2019. Deep Learning Recommendation Model for Personalization and Recommendation Systems. *arXiv preprint arXiv:1906.00091* (2019).
- [15] Junwei Pan, Jian Xu, Alfonso Lobos Ruiz, Wenliang Zhao, Shengjun Pan, Yu Sun, and Quan Lu. 2018. Field-weighted Factorization Machines for Click-Through Rate Prediction in Display Advertising. In *Proceedings of the 2018 World Wide Web Conference*. 1349–1357. <https://doi.org/10.1145/3178876.3186040>
- [16] Qi Pi, Xiaoqiang Zhu, Guorui Zhou, Yujing Zhang, Zhe Wang, Lejian Ren, Ying Fan, and Kun Gai. 2020. Search-based User Interest Modeling with Lifelong Sequential Behavior Data for Click-Through Rate Prediction. *arXiv preprint arXiv:2006.05639* (2020).
- [17] Yanru Qu, Han Cai, Kan Ren, Weinan Zhang, Yong Yu, Ying Wen, and Jun Wang. 2016. Product-based Neural Networks for User Response Prediction. In *2016 IEEE 16th International Conference on Data Mining (ICDM)*. 1149–1154.

- [18] Steffen Rendle. 2010. Factorization Machines. In *2010 IEEE International Conference on Data Mining (ICDM)*. IEEE, 995–1000. <https://doi.org/10.1109/ICDM.2010.127>
- [19] Alex Shtoff, Michael Viderman, et al. 2024. Low Rank Field-Weighted Factorization Machines for Low Latency Item Recommendation. In *Proceedings of the 18th ACM Conference on Recommender Systems (RecSys)*. <https://doi.org/10.1145/3640457.3688097>
- [20] Weiping Song, Chence Shi, Zhiping Xiao, Zhijian Duan, Yewen Xu, Ming Zhang, and Jian Tang. 2019. AutoInt: Automatic Feature Interaction Learning via Self-Attentive Neural Networks. In *Proceedings of the 28th ACM International Conference on Information and Knowledge Management (CIKM)*. 1161–1170. <https://doi.org/10.1145/3357384.3357925>
- [21] Fangye Wang, Yingxu Wang, Dongsheng Li, Hansu Gu, Tun Lu, Peng Zhang, and Ning Gu. 2023. Towards Deeper, Lighter and Interpretable Cross Network for CTR Prediction. In *Proceedings of the 32nd ACM International Conference on Information and Knowledge Management (CIKM)*.
- [22] Ruoxi Wang, Bin Fu, Gang Fu, and Mingliang Wang. 2017. Deep & Cross Network for Ad Click Predictions. In *Proceedings of the ADKDD'17 Workshop at KDD*. <https://doi.org/10.1145/3124749.3124754>
- [23] Ruoxi Wang, Rakesh Shivanna, Derek Cheng, Sagar Jain, Dong Lin, Lichan Hong, and Ed Chi. 2021. DCN V2: Improved Deep & Cross Network and Practical Lessons for Web-scale Learning to Rank Systems. In *Proceedings of the Web Conference 2021 (WWW)*. 1785–1797. <https://doi.org/10.1145/3442381.3450078>
- [24] Zhiqiang Wang, Qingyun She, and Junlin Zhang. 2021. MaskNet: Introducing Feature-Wise Multiplication to CTR Ranking Models by Instance-Guided Mask. In *DLP-KDD 2021 Workshop at KDD*.
- [25] Xue Xia, Pong Eksombatchai, Nikil Pancha, Dhruvil Deven Badani, Po-Wei Wang, Neng Gu, Saurabh Vishwas Joshi, Nazanin Farahpour, Zhiyuan Zhang, and Andrew Zhai. 2023. TransAct: Transformer-based Realtime User Action Model for Recommendation at Pinterest. In *Proceedings of the 29th ACM SIGKDD Conference on Knowledge Discovery and Data Mining (KDD)*. <https://doi.org/10.1145/3580305.3599918>
- [26] Xinyang Yi, Ji Yang, Lichan Hong, Derek Zhiyuan Cheng, Lukasz Heldt, Aditee Kumthekar, Zhe Zhao, Li Wei, and Ed Chi. 2019. Sampling-Bias-Corrected Neural Modeling for Large Corpus Item Recommendations. In *Proceedings of the 13th ACM Conference on Recommender Systems (RecSys)*. 269–277. <https://doi.org/10.1145/3298689.3346996>
- [27] Buyun Zhang, Liang Luo, Xi Liu, Jay Li, Zeliang Chen, Weilin Zhang, Xiaohan Wei, Yuchen Hao, Michael Tsang, Wenjun Wang, Yang Liu, Huayu Li, Yasmine Badr, Jongsoo Park, Jiyang Yang, Dheevatsa Mudigere, and Ellie Wen. 2022. DHEN: A Deep and Hierarchical Ensemble Network for Large-Scale Click-Through Rate Prediction. In *DLP-KDD 2022 Workshop at KDD*.
- [28] Guorui Zhou, Xiaoqiang Zhu, Chenru Song, Ying Fan, Han Zhu, Xiao Ma, Yanghui Yan, Junqi Jin, Han Li, and Kun Gai. 2018. Deep Interest Network for Click-Through Rate Prediction. In *Proceedings of the 24th ACM SIGKDD International Conference on Knowledge Discovery & Data Mining*. 1059–1068.
- [29] Jieming Zhu, Qinglin Jia, Guohao Cai, Quanyu Dai, Jingjie Li, Zhenhua Dong, Ruiming Tang, and Rui Zhang. 2023. FinalMLP: An Enhanced Two-Stream MLP Model for CTR Prediction. In *Proceedings of the AAAI Conference on Artificial Intelligence*.